Soft Control: A Novel Application of Internet of Things for Demand Side Management

Surya Chandan Dhulipala, Xin Li, Arturo Bretas, Dapeng Wu, Cody Ruben
Department of Electrical & Computer Engineering
University of Florida
Gainesville, FL
chandandhulipala@ufl.edu, shanelee@ufl.edu, arturo@ece.ufl.edu, dpwu@ufl.edu, cruben31@ufl.edu

***Abstract*—Demand side management (DSM) is the modulation of consumers' energy demand to ameliorate the power network at the consumer side. In case of contingency which leads to frequency falling below a preset value, traditional methods like load shedding, which de-energize one or more feeders, are implemented to prevent sustained interruptions. This approach is neither efficient nor reliable because this may lead to loss of energy to critical infrastructure and loss of distributed energy sources (DERs) injection. Implementation of home automation and communication systems in distribution networks enables optimization of energy consumption during a power system contingency. Energy Controllers (EC) can achieve fine adjustment of consumers' power consumption which can be used to selectively de-energize certain consumers, instead of a whole region. In this paper, a real-time centralized under-voltage event-based DSM approach called Soft Control (SC) that modulates energy consumption of each consumers' load utilizing Internet of Things (IoT) is presented. This DSM technique can be utilized for both active and passive distribution networks and is formulated as a utilization maximization problem. The performance of the proposed DSM approach is evaluated using the IEEE 16 bus system. The ease of implementation and computational efficiency highlight potential aspects for practical implementation.**

***Index Terms*—Internet of Things, demand side management, demand response, distributed generation, Markov process, smart grid, power quality.**

I. Introduction

During recent years, comprehensive studies have been made on the topic of Demand Side Management (DSM), which provides an efficient way to use load as an additional degree of freedom to improve system operation at consumer side. There is a need for efficient DSM strategies if a situation arises where the frequency falls below a certain preset value and frequency containment reserve is not enough to restore frequency and load shedding should be performed to avoid sustained interruption.

Several emergency control strategies have been proposed to prevent sustained system interruptions. One of such strategies is called 'system protection schemes' or 'wide-area protection schemes' to prevent voltage collapse [1] [2] [3] [4] [5]. Load shedding (LS) approaches are widely implemented as effective response strategies to tackle generation and load imbalance following a contingency. When system experiences an initial voltage drop that is too severe to overcome by load tap changers (LTC), DSM is a quick and effective solution against voltage collapse [6]. Some of the recent works explored the idea of DSM for under-frequency and under-voltage LS [7].

These LS approaches are not efficient and do not consider the advances in communication infrastructure due to advent of smart grid technologies [8]. Advances in sensor technology and Internet of Things (IoT) establishes a real-time communication between users, utilities and power equipment to achieve real-time, high-speed and two-way communication. These connections provide the capability to control equipment distributed over a large geographical area and selectively turn them ON/OFF when needed. Distributed energy sources (DERs) are capable of providing economic benefits during recovery from contingencies because locally generated energy can be consumed by local loads whenever it is available. The conventional LS approaches do not utilize these smart grid features and do not make optimal use of available energy while maintaining power quality in their design [8]. The latter is important because one wants to optimize the energy available in the event of an emergency.

Furthermore, conventional LS approaches shed load by switching off areas of a network in a controlled and planned manner [9]–[11]. Energy Controllers (ECs) at smart homes can modulate load consumption smoothly and selectively.

In this work, a SC DSM approach is presented. This DSM technique utilizes the smart grid infrastructure to make optimal use of available energy while maintaining power quality. We consider each customer is equipped with an EC with selective appliance control (*e.g.* home automation). Appliances with higher priority (or higher utility value) among all the appliances of a customer will be given priority. The proposed approach can be seen as a contribution to the incentive based centralized physical DR methods [12] [13] [14] and it fully utilizes DERs to help increase total economic benefits by improving customer utility and reducing power system losses. Furthermore, a better power quality is achieved with the SC approach when compared to conventional LS methods. The contribution of current work to state-of-art are:

- Control strategy for selective load modulation instead of deenergizing a whole distribution network area.
- Optimal use of energy available after an emergency event.
- Consideration of power quality in constrained DSM model.

2020 52nd North American Power Symposium (NAPS) | 978-1-7281-8192-9/21/$31.00 ©2021 IEEE | DOI: 10.1109/NAPS50074.2021.9449690

The remainder of this paper is organized as follows. Section II describes general aspects of the proposed DSM approach. In Section III, DSM problem is formulated as a weighted optimization problem. Specific SC approach implementation aspects are described in Section IV. A comparative study case is presented in Section V. Finally, some concluding remarks are presented in Section VI.

II. Soft Control for Demand Response: General Aspects

We assume that each customer is equipped with an EC which has a communication interface and ability to selectively control appliances.

A. Load Model

We define the set of customers $\mathcal{N}_c$ with cardinality $N = |\mathcal{N}_c|$ customers. For each customer $n \in \mathcal{N}_c$, let $\mathcal{A}_n$ denote the set of customer appliances. Each appliance has its own utility function which is a function of power supply. When power supply is not enough to run all appliances, only appliances with higher priority should work. For instance, low energy but critical devices would be given higher priority when energy supply is low.

To eliminate the non-linearity introduced by the constant P-Q load model in the solution of power flow (PF) equations, we utilize a voltage dependent load model [15] as:

$$\begin{aligned} \frac{P(V)}{P_0} &= C_Z\left(\frac{V}{V_0}\right)^2 + C_I\left(\frac{V}{V_0}\right) \\ \frac{Q(V)}{Q_0} &= C'_Z\left(\frac{V}{V_0}\right)^2 + C'_I\left(\frac{V}{V_0}\right) \end{aligned} \tag{1}$$

where P and Q are the load's active and reactive power consumption; V is the terminal voltage magnitude and P_0, Q_0, V_0 are the nominal values; constants C and C' are calculated by a curve-fitting procedure for different types of loads which satisfy $C_Z + C_I = 1$ and $C'_Z + C'_I = 1$.

B. Solar Forecasting: A Markov Chain Approach and Confidential Intervals

In order to forecast the amount of solar energy available for use after a contingency, we use Markov models to forecast and compute the transition probability from historical TMY3 data sets of Gainesville [16].

1) Markov chain model: A Markov chain is used to implement the stochastic element in the model, such as estimation of available wind and solar energy [17]. A Markov chain features two elements $(\mathcal{N}, \Pi)$, where $\mathcal{N} = \{1, 2, ..., N\}$ is the set of finite states and Π is a transition matrix, defining the probability of change between any two possible states. Let X_t be the state of the Markov chain at time t. The transition probability from state X_t to state X_{t+1} can be described as $\pi_{ij} = Pr\{X_{t+1} = j | X_t = i\}$. In our Markov model, we split maximum and minimum solar radiation value for each hour in N levels, which are labeled from level 1 to N. For each month of each year, the transition matrix Π is acquired from solar radiation data of the specific month from all historical

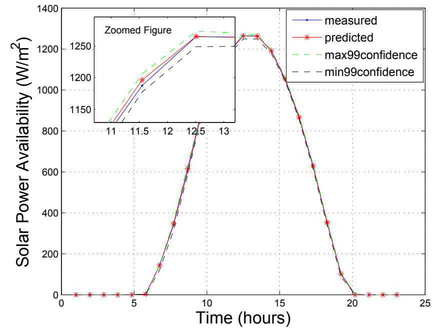

Fig. 1: Measured, forecast, minimum and maximum forecast value with 99% confidence interval

years. Thus, in this work a total of 12 Markov chain models, each corresponding to a month, are used.

2) Solar energy forecasting: Forecast of hourly solar radiation for each day is generated with the Markov chain corresponding to the month of that day and the historical solar radiation range for the corresponding hour. The forecast solar radiation $\hat{P}^S_{t+k}$ at time $t+k$ can be obtained by the transition probability value of the future state $\mathbb{E}[X^S_{t+k}|X^S_t = i]$ and the historical solar radiation range R^S_{t+k} at time $t+k$, where i is measured state at time t. Thus we have [17],

$$\hat{P}^S_{t+k} = \frac{1}{N} R^S_{t+k}\left(\mathbb{E}[X^S_{t+k}|X^S_t = i] - \frac{1}{2}\right). \tag{2}$$

Fig. 1 represents the data corresponding to a summer day, including the measured data P^S, the forecast data $\hat{P}^S$ using a Markov chain of 8 states and prediction horizon 1 min, the minimum and maximum values $\hat{P}^S_{min}$ and $\hat{P}^S_{max}$ of the 99% confidence interval for the forecast of power insolation.

C. Power Flow Equations

Assume the system admittance matrix $\bar{Y} = \bar{G} + j\bar{B}$, thus the power flow equation at node n could be written as,

$$\begin{aligned} \sum_{k=1}^{N}(\bar{G}_{n,k}V_k^{re} - \bar{B}_{n,k}V_k^{im}) &= I_{p,n} \\ \sum_{k=1}^{N}(\bar{G}_{n,k}V_k^{im} + \bar{B}_{n,k}V_k^{re}) &= I_{q,n} \end{aligned} \tag{3}$$

where N is the number of nodes; n and k are the two ends of line connecting nodes n and k; V^{re} and V^{im} are the real and imaginary part of nodal voltage; $I_{p,n}$ and $I_{q,n}$ are real and reactive part of corresponding nodal current injections at node n.

D. Appliances Utility

Each customer $n \in \mathcal{N}_c$ has a different utility function determined by the energy consumption of appliances. In this work, we choose quadratic utility functions [18]. These quadratic functions are non-decreasing and concave.

This work was supported by HDTRA1-14-1-0055 and NSF ECCS grants 1646229 and 1809739.

In [18], the quadratic utility function of the consumer $n \in N$ is described as:

$$U_n(P_n) = \begin{cases} \omega_n P_n - \dfrac{\alpha}{2} P_n^2, & \text{if } 0 \leq P_n \leq \dfrac{\omega_n}{\alpha} \\ \dfrac{\omega_n^2}{2\alpha}, & \text{if } P_n \geq \dfrac{\omega_n}{\alpha}. \end{cases} \tag{4}$$

where P_n is power supply for customer n, ω_n is a parameter which may vary among users and also at different times of the day, α is a pre-determined parameter, which represents utility gain characteristic of each load. For example, in utility models with distinct parameters, customers with life support devices would gain higher utility than those with only illuminating devices when they have the same amount of energy consumption.

III. Soft Control for Demand Response with IoT: Problem Formulation

In this section, we formulate an optimization problem to maximize consumer's utility while maintaining power quality. In the event of power system contingency, the total energy consumption should decrease to match the value of available power generation (total power from available substation P_{max} and solar plants $\hat{P}_t^S$ - distribution network technical power loss P_{loss}). To regain balance between energy generation and consumption, the adopted SC approach adjusts the power consumption in the period T of recovery.

A. Total Customers Utility Maximization

Assuming we have complete knowledge of customers' utility function (4), the most economical efficient load-shedding can be characterized as the maximum value of the following objective equation,

$$\underset{P_n}{\text{maximize}} \sum_{n \in \mathcal{N}} U_n(P_n) \tag{5}$$

where P_n is the power supplied at customers' bus n. We assume that each customer n will try his/her best to utilize the total amount of available energy supply, after the customer is affected by a contingency. Moreover those appliances which provide higher utility to customers (such as life support systems, lighting devices after sunset, etc.) will be turned on preferentially. Devices with similar utility are grouped to ensure that all the devices of a certain class (for instance: life support systems) in an area are ON if enough surplus energy was available. The strategy for grouping of devices into classes proposed in [13] was adopted in this work.

B. Weighted Optimization Problem Definition

We define our optimization problem for both active (with DG) and passive distribution systems using the weighted sum method for multi-objective optimization [19]. Utilization maximization and reduction of losses are the objectives in this strategy. Unlike traditional energy sources, renewable energy is an intermittent energy source. When a contingency occurs during daytime, solar plants in the affected area can help mitigate amount of load-shedding by providing energy locally. As solar availability fluctuates with time, we utilize its forecast value at the specific time t. We formulate the optimization problem in distribution networks with solar plant as:

$$\begin{aligned} \underset{P_n^t}{\text{maximize}} \; & w_u \sum_{n \in \mathcal{N}} U_n^t(P_n^t) + w_l P_{loss} \\ \text{subject to } & V_{min} \leq V_n^t \leq V_{max} \\ & \sum_{n=1}^{N} P_n^t \leq P_{max} - P_{loss}^t + \hat{P}_{t,min}^S \\ & \sum_{n=1}^{N} Q_n^t \leq Q_{max} - Q_{loss}^t + \hat{Q}_{t,min}^S \\ & I_{n,k,t}^2 \leq |I_{n,k}^{max}|^2 \end{aligned} \tag{6}$$

where w_u and w_l are the weights assigned to utility maximization and losses reduction respectively. P_n^t and Q_n^t are real power and reactive power injection on bus of customer n at current time t, P_{max} and Q_{max} are the maximum available real power and reactive power provided from feeders, P_{loss}^t and Q_{loss}^t are total real and reactive power loss at time t, $\hat{P}_{t,min}^S$ and $\hat{Q}_{t,min}^S$ are the confidence interval's lower bound of real and reactive power that could be provided by DER. V_n^t is the voltage magnitude of the bus. V_{min} and V_{max} establish the range of allowed voltage magnitude of each bus (e.g. $V_{min} = 0.90V_0$ and $V_{max} = 1.05V_0$). A slack was introduced to lower ANSI range to allow for extreme condition in emergency conditions. $I_{n,k,t}$ stands for current through line $n-k$ at time t, and it should not exceed power line flow limit of line $n-k$ $I_{n,k}^{max}$. Without loss of generality, passive distribution networks can also be described by making the power injection from DG equal to zero at each time slot.

In this work, a linear power flow formulation based on a voltage-dependent load model as described in II-A is adopted to solve the load flow [15]. The real power losses on line between node n and k are given by:

$$\begin{aligned} P_{n,k} =& u_{n,k} G_{n,k} [(V_{re,n} - V_{re,k})^2 \\ &+ (V_{im,n} - V_{im,k})^2]. \\ Q_{n,k} =& - u_{n,k} B_{n,k} [(V_{re,n} - V_{re,k})^2 \end{aligned} \tag{7}$$

where $V_{re,n}$ and $V_{im,n}$ are real part and imaginary part of the voltage, which can be calculated from linear power flow equation (3). $u_{n,k}$ is equal to zero if there is no line between nodes n and k. $G_{n,k}$ and and $B_{n,k}$ are the conductance and susceptance of power line $n-k$. The total network losses can be calculated by

$$\begin{aligned} P_{loss} &= \sum_{n,k,n<k} P_{n,k}. \\ Q_{loss} &= \sum_{n,k,n<k} Q_{n,k} \end{aligned} \tag{8}$$

Here the restriction $n < k$ in the summations is required to prevent adding the losses of the same line twice when there is a power line between node n and k (8).

This work was supported by HDTRA1-14-1-0055 and NSF ECCS grants 1646229 and 1809739.

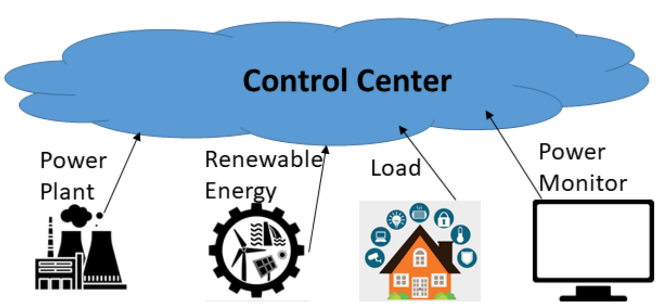

Fig. 2: System Diagram

IV. Soft Control for Demand Response with IoT: Implementation Aspects

Fig. 2 illustrates communication networks that support control loops between control centers and power system equipment. Home automation devices can adjust energy consumption of a consumer by turning selective appliances OFF or ON. The communication interface can be utilized to monitor status and control energy consumption of a consumer by collecting data and transferring control messages. One prominent system structure for future smart grid infrastructure is illustrated in Fig. 2. Sensors, meters, control devices and other devices communicate with each other via wireless network (e.g. 5GHz for short distance communication and 2.4GHz for long distance communication) in the same distribution network.

SC approach determines energy consumption of each consumer which helps to achieve maximum social benefit while maintaining balance between total energy generation and consumption. The procedure of control message generation is illustrated in the Fig. 3. During initialization stage, the latest distribution networks topology $u_{n,k}$, power line parameters $G_{n,k}$, $B_{n,k}$ and load profiles $C_{Z,n}$, $C_{I,n}$ are obtained from the database. When any of these parameters are updated in database, previous loaded data are substituted with the most recent data. When load-shedding request is triggered by the analysis of data from remote monitors, total available energy from substation P_{max} is loaded from database. The available energy $\hat{P}^S_{min,t}$ from DG at control operation time t can be obtained from the corresponding Markov model and historical data from the database.

With all the above parameters available, the utility maximization problem can be solved sequentially in time-steps for the recovery time. Since (6) is a convex program, it can be solved in a centralized way using convex programming techniques such as Interior Point Methods (IPM) [20]. Finally, control center periodically dispatches control messages with required energy consumption to the corresponding control device via communication networks. As long as power system is recovering from contingency, control center keeps broadcasting control messages to devices to optimize utility with updated parameters.

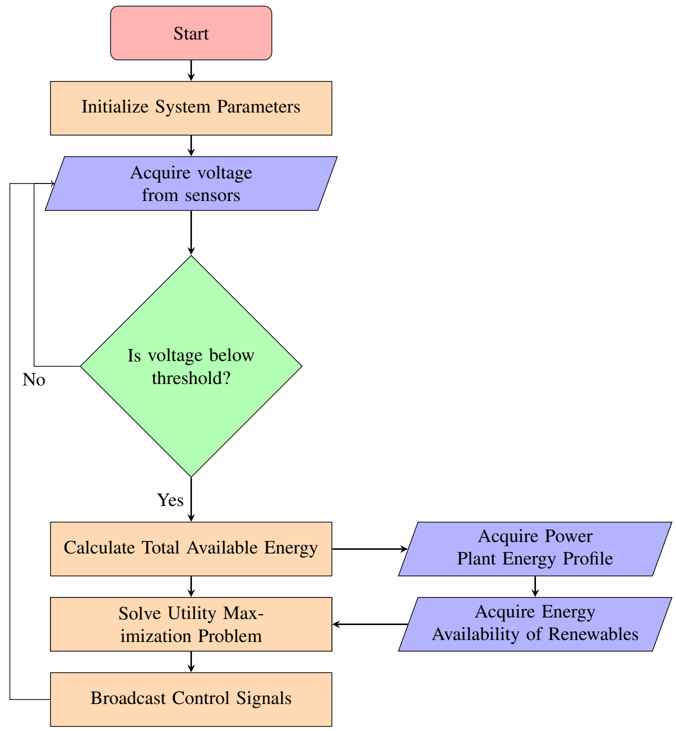

Fig. 3: Flowchart of Soft Control Approach

V. Experimental Evaluation

In this section, we compare the performance of the SC approach with an optimized adaptive load-shedding approach [8]. In order to make a fair comparison, we assume that the same amount of load (P_{shed}) is shed in both the approaches.

$$P_{shed} = \Delta P - P_{thr} \tag{9}$$

where ΔP is the total active power imbalance between generation and consumption, P_{thr} is the threshold value which stands for the maximum allowable amount of imbalance between generation and load to maintain frequency above a specific value.

A. Test Feeders and Load Profiles

We use the modified IEEE 16 node test feeder with 13 sectionalizing switches, 3 tie switches, overhead lines and 13 distribution buses in our simulations [21]. For presented approach evaluation considering an active distribution system, the 16 bus test feeder system is modified to include a 1.2 MW maximum solar farm on bus 12. The historical hourly insolation data is utilized to forecast power supply from solar farm at specific time in one day. We implemented the test feeder in Gridlab-D [22], a power distribution system simulation software. All customers' energy consumption can be controlled in our implementation, which simulates the operation of EC's after energy consumption control messages are received. All tie switches and sectionalizing switches are closed at the beginning of simulation. In our residential load model, we assume there are $N = 1300$ customers distributed

This work was supported by HDTRA1-14-1-0055 and NSF ECCS grants 1646229 and 1809739.

along the 13 nodes in 3 areas. Total power generation of 3 feeders is 5 MVA, which is balanced with total energy consumption. The appliances used by customers which are served by each bus are randomly allocated according to total power consumption in areas. In our experiment, we define 5 appliances classes and C_Z and C_I parameters of these classes are obtained from experimental measured real power P_0, reactive power Q_0 [15].

B. Case Study

In order to compare performance, a disturbance was simulated in the distribution network. To simulate a power system disturbance in the simulation platform, the amount of power injection in feeder-I is set to 0. This would lead to a sustained interruption event (here, an event is defined as sustained if it is greater than equal to five minutes in duration) then we calculate the total amount of load that should be shed according to (9). The adaptive LS approach drops loads of buses by ranking all buses of the system according to their VQ margins [8]. In our test, the ranking of buses in feeder-I area was: bus-4 $<$ bus-5 $<$ bus-6 $<$ bus-7. Thus loads shedding occurs in the order: bus-4, bus-5, bus-6, bus-7 until the total amount of load to be shed is satisfied. In contrast, our SC approach does not prompt a power outage to all consumers of the buses along feeder-I. The available power supply for each customer is calculated and a decision to turn on or off the devices is made by the controller. As the LS approach is not an appliance scheduling strategy, we randomize appliances' priorities for each customers and turn on as many as higher priority appliances as long as supply can meet the demand. In real world, the priority of a devices would be determined by its characteristic, consumer's behavior, time of the day, and other environmental factors. Thus, we think it is reasonable for our simulation to simplify this priority requirement.

1) Remainder Utility Value: Simulation results of weighted sum of utility and loss value for both adaptive LS approach and SC approach are shown in Fig.4, 5, 6 and 7 for various weights. We initiate the simulation at two different times: 12:00 A.M and 12:00 P.M and assume the disturbance event lasts for a full day. As power supply available from solar farm varies throughout the day, we run both control approaches every 30 minutes to follow the customer load changes. In contrast to adaptive LS, our approach is able to serve more consumers while maintaining power quality. When a disturbance event occurs at midnight in Fig. 4, both the approaches could not gain benefit from solar energy source. We drop loads of buses 4, 5, and 6 to reach the amount of LS requirement $P_{shed} = 1$MW with the adaptive LS approach. The adaptive LS approach could not exploit the intermittent nature of DER because the amount of load to be shed is determined using the energy available at that given instant. Our approach is able to fully utilize renewable energy when there is more energy available from the solar farm by turning on the devices according to customer priority. Fig. 6, shows that more utility is achieved by SC DSM approach when compared to adaptive LS approach when the disturbance event occurred at night

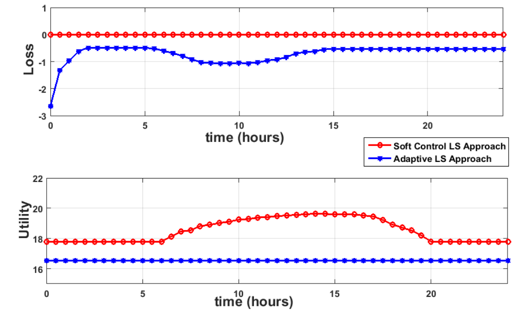

Fig. 4: Objective function value for various weights with additional solar energy from 12:00am

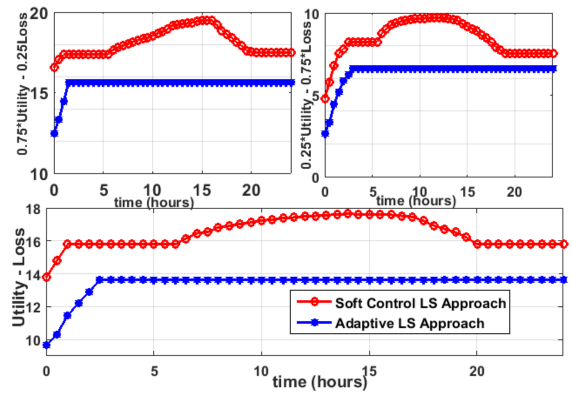

Fig. 5: Objective function value for various weights with additional solar energy from 12:00am

time. The same result was observed when the disturbance event occurs at daytime in Fig. 4. Fig. 4 and Fig. 6 illustrate the value of objective function when either losses or utility is considered when solar energy is available at 12:00 A.M and 12:00 P.M respectively. Fig. 5 and Fig. 7 illustrate the value of objective function for various weights w_u and w_l when solar energy is available at 12:00 A.M and 12:00 P.M respectively. In both scenarios, SC approach achieved higher utilization of the available resources while maintaining power consumption amount below available power generation and power flows through power lines below power line capacity. The adaptive LS approach focuses on dropping loads of buses without maintaining power quality. The distribution system with DERs in our approach outperforms the adaptive LS approach even if power flow constraint in lines is not considered in the adaptive LS approach.

2) Power Quality: Another advantage of our presented solution is improved voltage profile. As shown in Table. I, corresponding to event start times, the total number of customers $\sum_i N_i$ experiencing voltage deviations with magnitudes below 0.95 due to event is summed up. The simulation result shows that SC approach helps improving the SARFI$_x$ power quality and maintains better voltage profile.

This work was supported by HDTRA1-14-1-0055 and NSF ECCS grants 1646229 and 1809739.

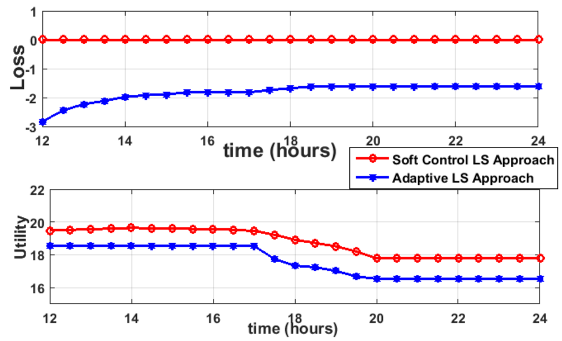

Fig. 6: Objective function value for various weights with additional solar energy from 12:00pm

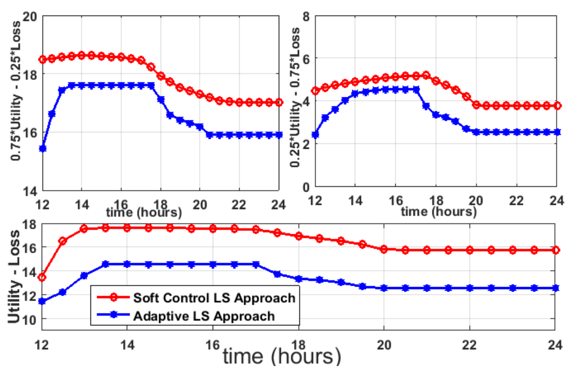

Fig. 7: Objective function value for various weights with additional solar energy from 12:00pm

VI. Conclusions

In this paper, a DSM approach is presented considering advancements in the smart grid infrastructure. The proposed method is based on utility maximization while maintaining power quality after a contingency. Control center calculates optimal energy consumption for each consumer utilizing the data from data centers. The results of simulation demonstrates that the SC DSM scheme is capable of maintaining higher aggregate utility of all consumers while efficiently maintaining power quality following a contingency compared to optimal adaptive load-shedding approach. The presented technique reduces technical losses on the lines and fully utilizes available energy from various energy sources.

TABLE I: System Average RMS Frequency Index$_{95}$

Event Time	Approaches	$\sum_i N_i$	N_T	$SARFI_{95}$
12:00am	Soft	0	1500	0
	Adaptive	567	1500	0.378
10:00am	Soft	0	1500	0
	Adaptive	466	1500	0.311
12:00pm	Soft	0	1500	0
	Adaptive	270	1500	0.180
4:00pm	Soft	0	1500	0
	Adaptive	363	1500	0.242

References

[1] M. Jonsson, *Protection Strategies to Mitigate Major Power Systems Breakdowns*. Chalmers University of Technology, Sweden, 2003.

[2] V. C. Nikolaidis and C. D. Vournas, "Design strategies for load-shedding schemes against voltage collapse in the hellenic system," *IEEE Transactions on Power Systems*, vol. 23, no. 2, pp. 582–591, May 2008.

[3] A. Wiszniewski, "New criteria of voltage stability margin for the purpose of load shedding," *IEEE Transactions on Power Delivery*, vol. 22, no. 3, pp. 1367–1371, July 2007.

[4] M. Larsson and D. Karlsson, "Coordinated system protection scheme against voltage collapse using heuristic search and predictive control," *IEEE Transactions on Power Systems*, vol. 18, no. 3, pp. 1001–1006, Aug 2003.

[5] Z. Feng, V. Ajjarapu, and D. J. Maratukulam, "A practical minimum load shedding strategy to mitigate voltage collapse," *IEEE Transactions on Power Systems*, vol. 13, no. 4, pp. 1285–1290, Nov 1998.

[6] T. Van Cutsem and C. Vournas, "Emergency voltage stability controls: an overview," in *IEEE Power Engineering Society General Meeting*. IEEE, 2007, pp. 1–10.

[7] J. Wang, H. Zhang, and Y. Zhou, "Intelligent under frequency and under voltage load shedding method based on the active participation of smart appliances," *IEEE Transactions on Smart Grid*, vol. 8, no. 1, pp. 353–361, Jan 2017.

[8] H. Seyedi and M. Sanaye-Pasand, "New centralised adaptive load-shedding algorithms to mitigate power system blackouts," *Generation, Transmission & Distribution, IET*, vol. 3, no. 1, pp. 99–114, 2009.

[9] C. W. Taylor, "Concepts of undervoltage load shedding for voltage stability," *IEEE Transactions on Power Delivery*, vol. 7, no. 2, pp. 480–488, April 1992.

[10] M. Jonsson, J. Daalder, and K. Walve, "An emergency strategy scheme based on conventional distance protection to avoid complete system collapse," in *2003 IEEE PES Transmission and Distribution Conference and Exposition (IEEE Cat. No.03CH37495)*, vol. 1, Sept 2003, pp. 315–319 Vol.1.

[11] B. Otomega and T. V. Cutsem, "Undervoltage load shedding using distributed controllers," *IEEE Transactions on Power Systems*, vol. 22, no. 4, pp. 1898–1907, Nov 2007.

[12] J. H. Dudley and M. A. Piette, "Solutions for summer electric power shortages: Demand response and its application in air conditioning and refrigerating systems," *Refrigeration, Air Conditioning, & Electric Power Machinery*, vol. 29, no. 1, pp. 1–4, 2008.

[13] P. Palensky and D. Dietrich, "Demand side management: Demand response, intelligent energy systems, and smart loads," *IEEE Transactions on Industrial Informatics*, vol. 7, no. 3, pp. 381–388, 2011.

[14] S. Lu, N. Samaan, R. Diao, M. Elizondo, C. Jin, E. Mayhorn, Y. Zhang, and H. Kirkham, "Centralized and decentralized control for demand response," in *Innovative Smart Grid Technologies (ISGT), 2011 IEEE PES*, 2011.

[15] J. R. Martí, H. Ahmadi, and L. Bashualdo, "Linear power-flow formulation based on a voltage-dependent load model," *IEEE Transactions on Power Delivery*, vol. 28, no. 3, pp. 1682–1690, 2013.

[16] S. Wilcox and W. Marion, *Users manual for TMY3 data sets*. National Renewable Energy Laboratory Golden, CO, 2008.

[17] J. Bright, C. Smith, P. Taylor, and R. Crook, "Stochastic generation of synthetic minutely irradiance time series derived from mean hourly weather observation data," *Solar Energy*, vol. 115, pp. 229–242, 2015.

[18] P. Samadi, A.-H. Mohsenian-Rad, R. Schober, V. W. Wong, and J. Jatskevich, "Optimal real-time pricing algorithm based on utility maximization for smart grid," in *IEEE International Conference on Smart Grid Communications (SmartGridComm)*. IEEE, 2010, pp. 415–420.

[19] R. T. Marler and J. S. Arora, "The weighted sum method for multi-objective optimization: new insights," *Structural and Multidisciplinary Optimization*, vol. 41, no. 6, pp. 853–862, Jun 2010. [Online]. Available: https://doi.org/10.1007/s00158-009-0460-7

[20] S. Boyd and L. Vandenberghe, *Convex optimization*. Cambridge University Press, 2004.

[21] S. Civanlar, J. Grainger, H. Yin, and S. Lee, "Distribution feeder reconfiguration for loss reduction," *IEEE Transactions on Power Delivery*, vol. 3, no. 3, 1988.

[22] D. P. Chassin, K. Schneider, and C. Gerkensmeyer, "GridLAB-D: An open-source power systems modeling and simulation environment," in *IEEE/PES Transmission and Distribution Conference and Exposition*, 2008.

This work was supported by HDTRA1-14-1-0055 and NSF ECCS grants 1646229 and 1809739.